

Direct Alkylation of Deoxyguanosine by Azaserine Leads to O^6 -Carboxymethyldeoxyguanosine

Susanne M. Geisen, Claudia M. N. Aloisi, Sabrina M. Huber, Emma S. Sandell, Nora A. Escher, and Shana J. Sturla*

Cite This: *Chem. Res. Toxicol.* 2021, 34, 1518–1529

Read Online

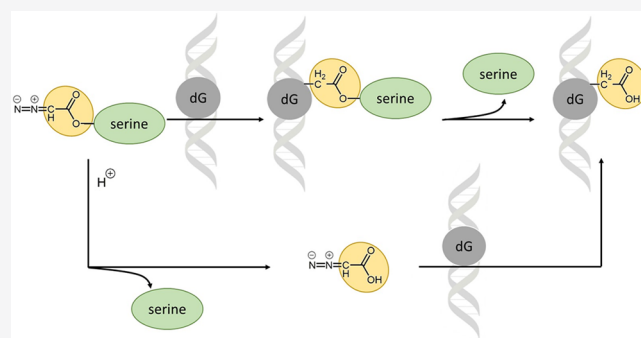
ACCESS |

Metrics & More

Article Recommendations

Supporting Information

ABSTRACT: The O^6 -alkylguanosine adduct O^6 -carboxymethyldeoxyguanosine (O^6 -CMdG) has been detected at elevated levels in blood and tissue samples from colorectal cancer patients and from healthy volunteers after consuming red meat. The diazo compound *L*-azaserine leads to the formation of O^6 -CMdG as well as the corresponding methyl adduct O^6 -methyldeoxyguanosine (O^6 -MedG) in cells and is therefore in wide use as a chemical probe in cellular studies concerning DNA damage and mutation. However, there remain knowledge gaps concerning the chemical basis of DNA adduct formation by *L*-azaserine. To characterize O^6 -CMdG formation by *L*-azaserine, we carried out a combination of chemical and enzymatic stability and reactivity studies supported by liquid chromatography tandem mass spectrometry for the simultaneous quantification of O^6 -CMdG and O^6 -MedG. We found that *L*-azaserine is stable under physiological and alkaline conditions as well as in active biological matrices but undergoes acid-catalyzed hydrolysis. We show, for the first time, that *L*-azaserine reacts directly with guanosine (dG) and oligonucleotides to form an O^6 -serine-CMdG (O^6 -Ser-CMdG) adduct. Moreover, by characterizing the reaction of dG with *L*-azaserine, we demonstrate that O^6 -Ser-CMdG forms as an intermediate that spontaneously decomposes to form O^6 -CMdG. Finally, we quantified levels of O^6 -CMdG and O^6 -MedG in a human cell line exposed to *L*-azaserine and found maximal adduct levels after 48 h. The findings of this work elucidate the chemical basis of how *L*-azaserine reacts with deoxyguanosine and support its use as a chemical probe for *N*-nitroso compound exposure in carcinogenesis research, particularly concerning the identification of pathways and factors that promote adduct formation.



INTRODUCTION

The structural integrity of nucleobases in DNA is essential for the correct functioning of cellular processes. The reaction of DNA with electrophilic exogenous and endogenous chemicals can result in DNA adducts that are mutagenic and initiate carcinogenesis. The DNA adducts O^6 -carboxymethyldeoxyguanosine (O^6 -CMdG) and O^6 -methyldeoxyguanosine (O^6 -MedG) are pro-mutagenic lesions of current interest in the context of colon carcinogenesis associated with meat consumption.^{1–5} Both adducts were elevated in blood and tissue samples from colorectal cancer patients.^{6–9} Further, O^6 -CMdG was detected in colonic exfoliated cells from human feces¹⁰ and in human blood samples from individuals on high-red-meat diets.¹¹ The association with meat, particularly red, was confirmed in other studies where O^6 -CMdG was detected at higher levels in tissues from volunteers with a high-red-meat diet compared to a vegetarian one¹² and in studies where digestion of red and white meat was modeled in vitro.^{13–15} The formation of O^6 -CMdG and O^6 -MedG was also observed after exposure of DNA to *N*-nitroso compounds (NOCs),^{11,16,17} which are present in red and cured meat¹⁸

or can be derived from nitrogenous dietary precursors via nitrite-mediated nitrosation of secondary amines that occurs largely endogenously.¹⁹ If unrepaired, the high miscoding potential of O^6 -MedG to pair with thymine results in GC → AT transition mutations upon replication.^{4,5} For O^6 -CMdG, the misincorporation of thymine, and to a smaller extent of adenine, could be demonstrated,^{20,21} therefore providing a mechanistic basis for the GC → AT transition and GC → TA transversion mutations found in the *p53* gene after treatment with a carboxymethylating agent and replication in yeast.²² Interestingly, these are also the two most common mutations found in colorectal cancer.^{22,23}

Carboxymethylating agents, such as compounds derived from *N*-carboxymethyl-NOCs and other chemical probes,²⁴

Received: October 30, 2020

Published: June 1, 2021



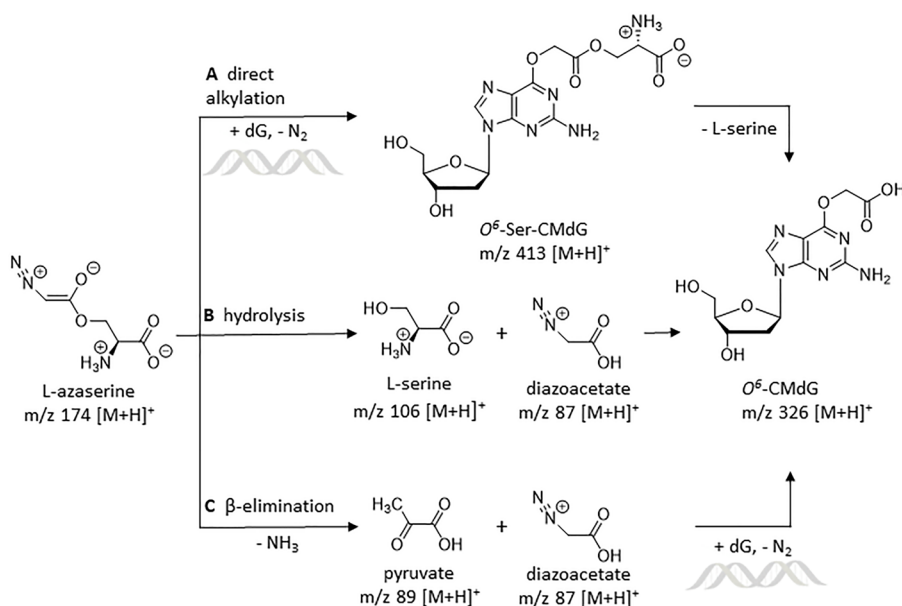


Figure 1. Proposed mechanisms for L-azaserine-induced O^6 -CMdG formation. (A) Nucleophilic attack of dG on L-azaserine results in an O^6 -Ser-CMdG intermediate followed by hydrolysis of L-serine to yield O^6 -CMdG. (B) L-Azaserine decomposes spontaneously to L-serine and diazoacetate, which subsequently carboxymethylates dG. (C) Enzymatic β -elimination of L-azaserine results in pyruvate and diazoacetate.

promote the formation of O^6 -CMdG (Figure 1) and to a lesser extent O^6 -MedG.^{11,17,25} For example, L-azaserine and potassium diazoacetate are commonly used to generate O^6 -CMdG and O^6 -MedG.^{8,10,17,26,27} In previous studies, potassium diazoacetate induced higher absolute levels of O^6 -CMdG and O^6 -MedG than L-azaserine, but the carboxymethyl:methyl ratio was lower for potassium diazoacetate.^{16,17} The average level of O^6 -CMdG and O^6 -MedG adducts after exposure to potassium diazoacetate was similar in cells and naked DNA, suggesting that no enzymatic activation is required for potassium diazoacetate. However, the high activity of potassium diazoacetate limits its use as a carboxymethylating agent, and no reproducible results were obtained in cells.¹⁰ Moreover, it is difficult to determine potassium diazoacetate concentration, due to its high instability and fast conversion during characterization. Hence, a nominal concentration is normally assumed based on quantitative production from alkaline hydrolysis of ethyldiazoacetate,^{10,28} but a true yield to our knowledge has never been determined. Based on technical limitations in the use of potassium diazoacetate, L-azaserine seems to be the preferred chemical for inducing O^6 -CMdG and O^6 -MedG, and exposure of cells to L-azaserine resulted in reproducible adduct levels.²⁷

L-Azaserine was discovered in 1954 as the active component of a crude filtrate from a culture of *Streptomyces* bacteria with antibiotic activity and potent antitumor activity in rodents.²⁹ It was positive in the Ames test and induced adenocarcinoma in rats³⁰ via the formation of DNA damage.³¹ The formation of O^6 -CMdG by L-azaserine was demonstrated by reaction with calf thymus DNA (ctDNA) and exposure in cells.^{16,17,26,27} Despite the long-standing knowledge that L-azaserine gives rise to O^6 -CMdG, details concerning the mechanism of this reaction remain limited.

It has been hypothesized that L-azaserine gives rise to carboxymethyl adducts by conversion to diazoacetate, which can carboxymethylate DNA (Figure 1). Two potential mechanisms for the conversion of L-azaserine in diazoacetate have been suggested: enzymatic β -elimination of L-azaserine to

diazoacetate and pyruvate (Figure 1C) or spontaneous hydrolysis to yield diazoacetate and L-serine (Figure 1B). Evidence for enzymatic β -elimination of L-azaserine was established using enzymatic extracts from mouse liver, and a stoichiometric relationship could be demonstrated for L-azaserine disappearance and glycolic acid, ammonia, and pyruvate formation, with the last two being the hydrolysis products of the β -elimination intermediate 2-aminoacrylate.³² The responsible enzyme was presumed to be a dehydrogenase.³³ Decomposition of L-azaserine to pyruvate and ammonia was also demonstrated in bicarbonate buffer, but only in the presence of pyridoxal ion as a cofactor. A pyridoxal ion-catalyzed β -elimination of L-azaserine via a Schiff base was suggested, resulting in diazoacetate and aminoacrylate that subsequent hydrolyses to pyruvate and ammonia.³⁴ However, the observation that O^6 -CMdG and O^6 -MedG form from L-azaserine and ctDNA in the absence of enzymes suggested an additional, nonenzymatic mechanism of L-azaserine breakdown that could yield DNA adducts. This mechanism has been proposed to involve spontaneous hydrolysis to yield serine and diazoacetate (Figure 1B).¹⁷ A further possibility is that L-azaserine may react directly with DNA and that subsequent hydrolysis yields O^6 -CMdG (Figure 1A).

The objective of this study was to elucidate the chemical mechanism of O^6 -CMdG formation by L-azaserine and establish a chemical basis for its use to address the corresponding DNA damage in cells. Thus, we evaluated the stability of L-azaserine under varying pH conditions and in the presence of active biological matrices. We characterized in detail the basis of O^6 -CMdG formation from the direct reaction of L-azaserine with guanosine and oligonucleotides. Finally, we quantified the formation of O^6 -CMdG and O^6 -MedG by L-azaserine in human colon epithelial cells (HCEC) on the basis of dose and time by establishing a mass spectrometry approach for the simultaneous and sensitive quantification of O^6 -CMdG and O^6 -MedG. The findings suggest a new direct reaction mechanism between L-azaserine and dG that gives rise to a O^6 -Ser-CMdG intermediate, which

undergoes spontaneous hydrolysis to form O^6 -CMdG. Further, the characterization of adduct formation in cells as a function of *L*-azaserine dose and time of exposure supports the use of *L*-azaserine as a chemical probe in future studies addressing biological consequences of O^6 -CMdG.

EXPERIMENTAL PROCEDURES

Materials. Potassium diazoacetate was synthesized via alkaline hydrolysis of ethyldiazoacetate as previously described, and neutral solutions for further usage were obtained by neutralizing with 0.1 M HCl.^{10,17,22} *L*-Azaserine was purchased from Abcam (Cambridge, UK) and purity confirmed by ¹H NMR. Ethyldiazoacetate was obtained from Pfaltz & Bauer Inc. (Waterbury, Connecticut), deoxyguanosine (dG) from Fluorochem (Hadfield, UK), and labeled ¹⁵N₅-dG from Cambridge Isotope Laboratories Inc., (Tewksbury, Massachusetts) and were used without further purification. *N*²-MedG standard was purchased from Carbosynth (Compton, UK). Oligonucleotide was ordered high-performance liquid chromatography (HPLC)-pure from Eurogentec. If not stated otherwise, all chemicals were purchased from Sigma-Aldrich (Buchs, Switzerland) and used without further purification. Milli-Q water was from a Millipore Synergy UV device. Mobile phases for liquid chromatography (LC) were obtained from Sigma-Aldrich (Buchs, Switzerland), and mobile phases for LC coupled with mass spectrometry (LC-MS) were purchased from Biosolve Chimie (Dieuze, France). All media and buffers for cell culture were purchased from Invitrogen (Carlsbad, California). HCEC-1CT cell lines were kindly provided by Prof J.W. Shay (University of Texas, USA).³⁵ NMR analysis was performed on a Bruker Biospin 400 MHz NMR instrument (Bruker, Billerica, Massachusetts), and chemical shifts are reported in parts per million (ppm, δ) referenced to the chemical shift of the respective solvent. NMR solvents were purchased from Sigma-Aldrich (Buchs, Switzerland). NMR files were evaluated by Mnova version 11 (Mestrelab Research, Santiago de Compostela, Spain). Reversed-phase HPLC analysis was performed on either an Agilent 1100 or 1200 Series HPLC (Agilent Technologies, Santa Clara, California).

Data were analyzed and plotted using GraphPad Prism, Version 8 (GraphPad Software Inc., San Diego, California). Applied statistical tests are specified for each data set in the corresponding figure caption.

pH Stability of *L*-Azaserine. *L*-Azaserine (25 mM) was dissolved in 500–980 μ L of 0.1 M buffer solutions at a pH ranging from pH 2 to 11: pH 2, 2.4, and 3.4 glycine-HCl buffer, pH 5.8 sodium phosphate, pH 7.2 sodium phosphate buffer, pH 8.5 carbonate buffer, and pH 10.5 tris-buffer. Solutions were analyzed by reversed-phase HPLC with a diode array detector set to monitor absorbance at $\lambda = 254$ nm (*L*-azaserine) and 210 nm (serine, pyruvate) on a Luna C18 column, 4.6 \times 250 mm, particle size 5 μ m, and pore size 100 Å (Phenomenex, Torrance, California) using H₂O as mobile phase A and ACN as mobile phase B. Chromatographic separation was achieved by an initial isocratic hold at 100% A for 5 min, followed by a gradient to 40% B in 10 min at a flow rate of 1 mL/min. Injection volume was 10 μ L. The starting concentration of *L*-azaserine was chosen to allow for detection of 0.5% and quantification of 2% hydrolysis to *L*-serine (LOQ 0.5 mM *L*-serine). Each sample (pH 2–11) was analyzed every 3 h for a total of 120 h. The analytical method was shortened for samples at pH 2–5.8 to an isocratic hold at 100% A for 6.0 min. *L*-Serine eluted at retention time 2.6 min, pyruvate at 2.9 min, and *L*-azaserine at 3.8 min. A calibration curve for *L*-azaserine and *L*-serine from 0.5, 1, 6, 12, 25, and 50 mM was analyzed.

Activity of Whole Cell Lysate toward *L*-Azaserine. *L*-Azaserine (5 μ L of 2 mM stock solution) was added to freshly prepared whole cell lysate (100 μ L) derived from human lung epithelial cells (BEAS-2B cells, ATCC CRL-9609) cultured in bronchial epithelial basal medium (BEBM, Lonza) at 37 °C in 5% CO₂ atmosphere. To obtain the lysate, growth medium was removed when the cells reached a confluency of ~80%, and 1 \times DPBS (10 mL) was added to wash the cells. Per 100 mm cell culture dish, 1 mL of CellLytic M (Sigma, C2978) was added followed by incubation at room temperature for

30 min on a shaker. Cell lysate was collected using a cell scraper and transferred into a 1.5 mL Eppendorf tube for immediate use. The mixture was incubated at 37 °C between 30 min and 24 h. After incubation, the mixture was loaded onto a prewashed 10 kDa MWCO filter unit (VWR, prewashed with H₂O (300 μ L) by centrifugation at 12,000g for 5 min) and centrifuged at 12,000g for 10 min. The flow through was loaded onto a Phenomenex Strata-X 33 μ m Polymeric Reversed Phase 30 mg/1 mL SPE column that was prewashed with 2 \times 1 mL MeOH followed by 2 \times 1 mL H₂O. The *L*-azaserine-containing fraction was eluted using 400 μ L of H₂O, concentrated to dryness by vacuum centrifugation and redissolved in 50 μ L H₂O for HPLC analysis using the identical method as described in the pH Stability of *L*-Azaserine section. Results are shown in Figure S1A. As a positive control, fluorescein diacetate (FDA) was also tested as a substrate. Stock solutions (20 mg/mL in acetone) were stored at –20 °C, and immediately before use, an aliquot of FDA stock solution was diluted in acetone to a final concentration of 2 mg/mL. FDA (2 μ L of 2 mg/mL acetone solution) was added to fresh cell lysate (400 μ L) or to CellLytic M (400 μ L) to obtain a final FDA concentration of 24 μ M. The resulting mixtures were allowed to react at room temperature for 2 h and applied to prewashed 10 kDa MWCO filter units and centrifuged (12,000g for 10 min). The 50 μ L aliquots of the flow throughs were loaded on a black 96 half-well plate for analysis. The experiment was performed three times.

To quantify the amount of FDA converted to fluorescein, a stock solution was prepared fresh at a concentration of 2 mg/mL in acetone. This stock solution was used to generate a fluorescein calibration line in CellLytic M with fluorescein concentrations of 75 μ M, 50 μ M, 25 μ M, 10 μ M, 5 μ M, 1 μ M, and 0.5 μ M. The 50 μ L aliquots (triplicates) of each concentration were loaded on a black 96 half-well plate for analysis. Fluorescence measurements were acquired on an Infinite M200 Pro plate reader from Tecan at 18 °C using excitation wavelength of 490 nm and an emission wavelength of 525 nm. No fluorescence readout was obtained for the FDA in CellLytic control, confirming that there is no spontaneous hydrolysis of FDA occurring.

Incubation of *L*-Azaserine with Porcine Liver Esterase. Lyophilized powder of porcine liver esterase (Sigma, E3019) was reconstituted in 10 mM borate buffer pH 8.0 at a concentration of 40 mU/ μ L. *L*-Azaserine (100 μ M) in 10 mM borate buffer pH 8.0 was incubated at 37 °C with varying amounts of porcine liver esterase (0.04–4 U) between 30 min and 24 h. After incubation, the esterase was removed by filtration over a 10 kDa MWCO filter unit at 12,000g for 5 min. The flow through was directly used for HPLC quantification of *L*-azaserine using the identical method as described in the pH Stability of *L*-Azaserine section. Results are shown in Figure S1B. FDA was tested as positive control as described in Activity of Whole Cell Lysate toward *L*-Azaserine section.

Reaction of an Oligonucleotide with *L*-Azaserine. A 9-mer oligonucleotide (TTTTGTTTT, 5 mM) was allowed to react with *L*-azaserine (50 mM) in 1 \times sodium phosphate buffer (20 μ L) at 37 °C for 24 h. The resulting mixture (20 μ L) was directly analyzed by reversed-phase HPLC with a diode array detector set to monitor absorbance at $\lambda = 260$ nm on a Clarity oligo-RP column, 250 \times 4.6 mm, particle size 5 μ m, pore size 110 Å (Phenomenex, Torrance, California) using TEAA 50 mM as mobile phase A and acetonitrile (ACN) as mobile phase B. Chromatographic separation was achieved by a gradient from 92% A to 85% A in 30 min at a flow rate of 1 mL/min. The unreacted oligonucleotide eluted with a retention time of 21 min, followed by three small peaks with retention times 21.5, 22.0, and 22.7 min (Figure S2A). Fractions of these peaks were collected and further analyzed by electrospray ionization mass spectrometry on a Velos Linear Ion Trap (Thermo Scientific, Waltham, Massachusetts). The electrospray mass spectrum for the material that eluted at 21.96 min in the UV-chromatogram corresponded to the anticipated *m/z* value of the electrospray ionization mass for the O^6 -Ser-CMG-oligonucleotide (2845.46, Figure S2C). To verify the structure and sequence, this material was further fragmented to obtain its MS2 mass spectrum. The collision energy was set at 30 with parent *m/z* 948, which predominantly generated a-B and w type fragment ions (Figure

S2B). The CID mass fragments corresponded to the calculated mass fragments of the O^6 -Ser-CMG-oligonucleotide, indicating the anticipated sequence context and the serine modification to be on guanine. HRMS was calculated for TTTT-G-TTTT: $[M - H]^-$ m/z 2699.813, found 674.12, 898.994, 1348.94, Magtran deconvolution 2700.26, TTTT- O^6 -CMG-TTTT: $[M - H]^-$ m/z 2759.7, found 688.32, 918.46, 1377.94, Magtran deconvolution 2758.48, TTTT- O^6 -Ser-CMG-TTTT: $[M - H]^-$ m/z 2846.69, found 568.044, 710.483, 947.45, 1421.45, Magtran deconvolution 2845.46

Preparation of Standards for Mass Spectrometry. O^6 -CMdG was prepared by the copper carbene-based method described by Geigle et al.³⁶ In short, 2.5 mg (9.35 μ mol) of dG was allowed to react with 10.7 mg (93.5 μ mol) of ethyldiazoacetate in the presence of 300 μ g (1.87 μ mol) $CuSO_4$. O^6 -CMdG was obtained by alkaline hydrolysis followed by reversed-phase HPLC purification with a diode array detector set to monitor absorbance at $\lambda = 280$ and 250 nm on a Luna C18 column, 4.6 \times 250 mm, particle size 5 μ m, pore size 100 \AA (Phenomenex, Torrance, California) using 0.1% HOAc as mobile phase A and ACN as mobile phase B. Chromatographic separation was achieved by an initial isocratic hold at 100% A for 10 min, followed by a gradient to 16% B in 45 min at a flow rate of 1 mL/min. Injection volume was 20 μ L. The product (RT 41.3 min, $\lambda = 280$, 250 nm) was obtained in 40% yield as a white powder. HRMS (ESI) calculated for $C_{12}H_{15}N_5O_6$: $[M + H]^+$ m/z 326.1101, found 326.1095, MS^2 calculated for $C_7H_7N_5O_3$: $[M + H - Gua]^+$ m/z 210.0628, found 210.0617. 1H NMR (Figure S3) matched published data.¹⁶ $^{15}N_5$ - O^6 -CMdG was prepared by the same protocol using 2.5 mg (9.35 μ mol) of dG $^{15}N_5$ -dG as starting material, yielding 1 mg (40% yield) of a white powder of $^{15}N_5$ - O^6 -CMdG. HRMS (ESI) calculated for $C_{12}H_{15}^{15}N_5O_6$: $[M + H]^+$ m/z 331.0952, found 331.0944, MS^2 calculated for $C_7H_7^{15}N_5O_3$: $[M + H - Gua]^+$ m/z 215.0479, found 215.0469 $[M + H - Gua]^+$.

O^6 -MedG was synthesized by the method reported by Reza et al.³⁷ In short, 0.57 g (2 mmol) dG was allowed to react in 10 mL of pyridine with 4.3 g (79.6 mmol) of sodium methoxide in 300 mL of MeOH. The product was purified by reversed-phase HPLC with a diode array detector set to monitor absorbance at $\lambda = 260$ nm on a Luna C18 column 10 \times 250 mm, particle size 5 μ m, pore size 100 \AA (Phenomenex, Torrance, California) using 5% ACN in H_2O as mobile phase A and ACN as mobile phase B. Chromatographic separation was achieved by an initial isocratic hold at 100% A for 15 min, followed by gradient to 35% B in 10 min at a flow rate of 2 mL/min. Injection volume was 200 μ L. Product (RT 20.7 min, $\lambda = 260$ nm) was obtained in a 60% yield as a light yellow powder. HRMS (ESI) calculated for $C_{11}H_{13}N_5O_4$: $[M + H]^+$ m/z 282.1202, found 282.1197, MS^2 calculated for $C_6H_7N_5O$: $[M + H - Gua]^+$ m/z 166.0729, found 166.0715. 1H NMR (Figure S4) matched the published data.³⁷ D_3 - O^6 -MedG was synthesized accordingly with 0.19 g (0.67 mmol) of dG and 1.51 g (26.5 mmol) of D_3 -sodium methoxide in 100 mL MeOD (both Armar chemicals, Switzerland). Product was purified by reversed-phase LC as described for unlabeled O^6 -MedG and obtained as a light-yellow powder in 60% yield. HRMS (ESI) calculated for $C_{11}H_{12}D_3N_5O_4$: $[M + H]^+$ m/z 285.1391, found 285.1383, MS^2 calculated for $C_6H_5D_3N_5O$: $[M + H - Gua]^+$ m/z 169.0918, found 169.0904. We did not observe any D/H exchange by analyzing a 100 nM D_3 - O^6 -MedG standard solution by nanoLC-ESI-HRMS² and following the intensity in the extracted ion chromatograms (XICs) for D_3 - O^6 -MedG (m/z 285.1383 $[M + H]^+$) and O^6 -MedG (m/z 282.1197 $[M + H]^+$, not detectable (nd)) over time of the analysis.

Reaction of dG with L-Azaserine. dG (5 μ M in 500 μ L Milli-Q or tris-buffer (10 mM) containing 2 mM $MgCl_2$, at pH 7, 8, 9, and 10.6) was combined with L-azaserine or potassium diazoacetate (5 mM), and the reaction mixture was stirred for 0.5, 1, 2, 3, and 24 h at 37 $^\circ$ C. After the indicated time, samples were processed for quantification of O^6 -CMdG and O^6 -MedG and analyzed by nanoLC-ESI-HRMS², as described in the detailed method validated for analysis of cell samples elaborated below, with the following changes: Trapping time was set to 0.1 min. Resolution was set to 60 K for the orbitrap mass analyzer in MS^1 , 68–444 m/z , and 1 microscan.

Target inclusion list was expanded to include O^6 -Ser-CMdG m/z 413.1421 $[M + H]^+$, O^6 -Ser-CMG m/z 297.0947 $[M + H]^+$, L-azaserine m/z 174.0515 $[M + H]^+$, serine m/z 106.0504 $[M + H]^+$, and dG m/z 268.1046 $[M + H]^+$. The mass tolerance was set to ± 50 ppm. Fragmentation of a O^6 -Ser-CMdG was targeted in MS^2 XICs with neutral loss of dR, O^6 -Ser-CMG m/z 297.0947 $[M + H - dR]^+$, and serine fragment,^{38–40} with m/z 251.0893 $[M + H - (dR + H_2O + CO)]^+$. Mass tolerance for all XICs was ± 10 ppm.

Synthesis of O^6 -Ser-CMdG. Four mM dG was dissolved in 1200 μ L of 0.1 M sodium phosphate buffer at pH 7.2. Twenty-five mM L-azaserine was added, and the mixture was allowed to react at 22 $^\circ$ C for 120 h while being continuously analyzed by reversed-phase HPLC with a diode array detector set to monitor absorbance at $\lambda = 254$ nm (L-azaserine, dG, G, O^6 -CMdG, O^6 -Ser-CMdG), 210 nm (L-serine), and 280 nm (O^6 -CMdG, O^6 -Ser-CMdG) on a Luna C18 column, 4.6 \times 250 mm, particle size 5 μ m, pore size 100 \AA (Phenomenex, Torrance, California) using H_2O as mobile phase A and ACN as mobile phase B. Chromatographic separation was achieved by an initial isocratic hold at 100% A for 5 min, followed by a gradient to 45% B in 45 min at a flow rate of 1 mL/min. Injection volume was 10 μ L. All eluting peaks were identified by m/z on a Velos Linear Ion Trap (Thermo Scientific, Waltham, Massachusetts) and in case of L-azaserine, dG, guanine, and L-serine with coelution of respective standards and corresponding DAD spectrum. L-Azaserine eluted at retention time 3.9 min (m/z 174), dG at 16.8 min (m/z 268), L-serine at 2.8 min (m/z 106), and guanine at 11.4 min (m/z 152). A peak at retention time 7.9 min had m/z 297 matching the calculated mass for Ser-G, while the peak of interest eluted at retention time of 18.7 min with m/z 413 as calculated for O^6 -Ser-CMdG (Figure S5A). This peak was collected over 200 runs and characterized. HRMS was calculated for $C_{15}H_{20}N_6O_8$: $[M + H]^+$ m/z 413.1421, found 413.1411 (Figure S5B), and MS^2 was calculated for $C_{10}H_{12}N_6O_5$: $[M + H - Gua]^+$ m/z 297.0947, found 297.0938. 1H NMR in deuterium oxide confirmed presence of O^6 -Ser-CMdG (Figure S5C). 1H NMR (400 MHz, deuterium oxide) δ 8.14 (s, 1H, Ar-H), 6.38 (t, $J = 8.2$ Hz, 1H, 1'-H), 5.07 (s, 1H, NH_2 -CH), 4.83–4.81 (m, 2H, O- CH_2 -COO), 4.67–4.62 (m, 1H, 4'-H), 4.18–4.13 (m, 1H, 3'-H), 3.93–3.84 (m, 2H, O- CH_2 - CNH_2), 3.83–3.74 (m, 2H, 5'-H), 2.84 (dt, $J = 14.7$, 7.4 Hz, 1H, 2'-H), 2.57–2.46 (m, 1H, 2'-H).

Hydrolysis of O^6 -Ser-CMdG. O^6 -Ser-CMdG was dissolved in 0.1 M phosphate buffer at pH 7.2, and the solution was analyzed by reversed-phase HPLC every hour for a total of 30 h and peaks identified as described above but using HOAc as mobile phase A and a gradient consisting of an initial isocratic hold for 10 min at 100% A, followed by a gradient to 16% B in 45 min. A product eluting at 42.5 min (Figure S6A) was isolated and confirmed to be O^6 -CMdG on the basis of 1H NMR (Figure S6C) and HRMS (ESI) calculated for $C_{12}H_{15}N_5O_6$: $[M + H]^+$ 326.1101, found 326.1094, matching the authentic standard.

Cell Culture of HCEC Cells and L-Azaserine Exposure. Cells were maintained as monolayers in 10 cm dishes in a humidified, 5% CO_2 atmosphere at 37 $^\circ$ C. Media consisted of 80% DMEM and 20% M199 Earle's salt medium, supplemented with 2% Hyclone fetal bovine serum (Hyclone Laboratories Inc., San Angelo, Texas), 25 ng/L epidermal growth factor, 1 μ g/L hydrocortisone, 10 μ g/L insulin, 2 μ g/L transferrin, 50 μ g/L gentamycin, and 0.9 ng/L sodium selenite. Cells were regularly confirmed to be mycoplasma free using the MycoAlert Kit (Lonza, Basel, Switzerland).⁴¹ L-Azaserine stock solutions were prepared in Milli-Q water. O^6 -Benzylguanine (O^6 -BG) stock solutions were prepared in dimethyl sulfoxide (DMSO), and the final concentration of DMSO was 0.1%. To assess cell viability, cells were seeded in 96-well plates at a density of 1×10^4 and exposed to increasing L-azaserine concentrations (0, 1, 10, 50, 250, 750, 1000, 2500 μ M) for 120 h. Cells were exposed to TritonX (Sigma-Aldrich, Buchs, Switzerland) as a positive control for cytotoxicity. Cell survival was measured using the CellTiterGlo assay (Promega, Madison, Wisconsin) following the manufacturer's instructions.⁴²

For DNA adduct analysis, cells were seeded in 10 cm dishes at a density of 2×10^6 . Cells were exposed to 0, 125, 250, 500, and 1000

μM L-azaserine for 4 h to evaluate the dose–response relationship and with 500 μM L-azaserine for 0.5, 4, 10, 24, 48, 72, 96, and 120 h to determine the time-dependent O^6 -CMdG and O^6 -MedG formation. Cell viability, dose–response, and time course studies were each performed three independent times.

DNA Isolation and Sample Preparation for Adduct Analysis by Mass Spectrometry. DNA was isolated from cell pellets using the QIAamp DNA Mini Kit (©QIAGEN, Switzerland). Extracted and dried DNA (20 μg) was dissolved in buffer (10 μL , 10 mM Tris pH 7, 2 mM MgCl_2). To this sample was added 50 μL of a master mix solution comprised of 2.5 U/ μg DNA benzonase, 3 mU/ μg DNA phosphodiesterase I, 2 U/ μg DNA alkaline phosphatase, 2 nM D_3 - O^6 -MedG and 4 nM $^{15}\text{N}_5$ - O^6 -CMdG in the aforementioned buffer. A solution of ctDNA (20 μg in 10 μL buffer) and a blank sample (10 μL buffer) were combined with 50 μL of the master mix as controls for DNA digestion and background signal, respectively. Following the digestion, MS grade H_2O (350 μL) was added to the sample (total volume 410 μL), and enzymes were removed by molecular weight filtration with a cutoff of 10 kDa (VWR, Radnor, Pennsylvania). An aliquot (60 μL) of the resulting solution was removed for dG quantification by HPLC (described below). Samples were concentrated to dryness in a Thermo Scientific Savant Universal SpeedVac Vacuum system, resuspended in 200 μL MS grade H_2O + 0.1% formic acid (FA), and further processed by solid-phase extraction on a C18 cartridge, Sep-Pak Vac 1 cm^3 (50 mg) (Waters, Milford, Massachusetts) using MS grade CH_3OH , CH_3OH + FA, and H_2O . Cartridges were washed with 2×1 mL CH_3OH and 1 mL CH_3OH + 0.1% FA followed by 2×1 mL H_2O + 0.1% FA. The samples were loaded on the cartridge, washed with 2×1 mL H_2O + 0.1% FA and 1 mL 3% CH_3OH , and eluted with 2×500 μL of 80% CH_3OH in H_2O . The eluted fractions were dried under vacuum and dissolved in 10 μL H_2O for subsequent MS analysis.

High-Resolution Mass Spectrometry Method for Simultaneous Quantification of O^6 -CMdG and O^6 -MedG. Simultaneous quantification of O^6 -CMdG and O^6 -MedG was achieved on an Orbitrap Fusion Lumos (Thermo Scientific, Waltham, Massachusetts) equipped with a nano electrospray ionization source and a nanoAcquity UPLC M-class system (Waters, Milford, Massachusetts). Liquid chromatography was performed with an Acquity UPLC M-Class Symmetry C18 Trap column (100 \AA , 5 μm , 180 $\mu\text{m} \times 20$ mm) and an Acquity UPLC M-Class HSS T3 column (100 \AA , 1.8 μm , 75 $\mu\text{m} \times 250$ mm) at a column temperature of 40 $^\circ\text{C}$. The sample loop volume was 5 μL , with an injection volume of 2 μL . Mobile phases A and B consisted of mass spectrometry grade H_2O with 0.1% FA and ACN with 0.1% FA, respectively (Biosolve Chimie, Dieuze, France). The chromatographic method included trapping for 0.5 min at 99.5% A at a flow rate of 15 $\mu\text{L}/\text{min}$. The chromatographic separation was achieved by a 1 min hold at 3% B, followed by a linear gradient from 3% to 45% B over 19 min, at a flow rate of 0.3 $\mu\text{L}/\text{min}$. Nano electrospray ionization was used in positive mode, 2.2 kV at 270 $^\circ\text{C}$. Mass spectrometry-based detection was performed in parallel reaction monitoring (PRM) with higher-energy collisional dissociation in orbitrap technology (HCD-OT) detection mode with the following settings: The RF lens was set to 35%. Resolution of the orbitrap was set to 120 K in MS^1 , 160–400 m/z , and 1 microscan. AGC target was set to 4×10^5 with a maximum injection time of 100 ms. Targeted inclusion list was comprised of O^6 -CMdG with m/z 326.1096 $[\text{M} + \text{H}]^+$, heavy $^{15}\text{N}_5$ - O^6 -CMdG with m/z 331.0946 $[\text{M} + \text{H}]^+$, O^6 -MedG with m/z 282.1995 $[\text{M} + \text{H}]^+$, and heavy D_3 - O^6 -MedG with m/z 285.1384 $[\text{M} + \text{H}]^+$. The mass tolerance was set to ± 25 ppm. Isolation for MS^2 was performed in the quadrupole with an isolation window of 1.6 m/z and the first mass set to 140 m/z . HCD was used for fragmentation with a collision energy of 25%. Fragments were detected in the orbitrap with a resolution of 60 K. The AGC target was set to 5×10^4 with a maximum injection time of 118 ms. For quantification, neutral loss of deoxyribose was targeted in XICs using O^6 -CMG m/z 210.0622 $[\text{M} + \text{H} - \text{Gua}]^+$, heavy $^{15}\text{N}_5$ - O^6 -CMG m/z 215.0472 $[\text{M} + \text{H} - \text{Gua}]^+$, O^6 -MeG m/z 166.0722 $[\text{M} + \text{H} - \text{Gua}]^+$, and heavy D_3 - O^6 -MeG m/z 169.0911 $[\text{M} + \text{H} - \text{Gua}]^+$ with a mass tolerance of ± 10 ppm. Calibration standards containing 0.5, 1, 5, 10,

25, 50, and 100 nM of O^6 -CMdG and O^6 -MedG standards undergoing sample preparation served for quantification (Figure S7).

Specificity was guaranteed by processing a blank sample for each analysis and selectivity by coelution with internal standards and accurate parent and fragment mass. Pure standards were used to determine the limit of detection (LOD) and limit of quantification (LOQ) defined as the amount of analyte generating a signal-to-noise ratio (S/N) of 3 or 10 in the XICs. LOD ($S/N > 3$) was 5 pM (10 amol) and 1 pM (2 amol) for O^6 -CMdG and O^6 -MedG, respectively, and LOQ ($S/N > 10$) was 10 pM (20 amol) for both adducts. We further assessed LOQ in matrix, intra- and interday accuracy (expressed as % recovery), and precision (expressed as the relative standard deviation, RSD %) using quality control samples consisting of calf thymus DNA (ctDNA, 15 μg) or HCEC genomic DNA (15 μg) spiked with increasing amounts of O^6 -CMdG and O^6 -MedG (0.01, 0.05, 0.1, 1.0, 10, 50, 100 and 200 nM). LOQ in matrix was determined to be 50 pM (100 amol) for O^6 -CMdG and O^6 -MedG. The precision and accuracy for the measurement of O^6 -CMdG and O^6 -MedG in ctDNA and HCEC genomic DNA as matrix (Table S1) had a relative standard deviation (RSD) ranging from 1.7 to 25.6% (O^6 -CMdG) or 0.8 to 23.5% (O^6 -MedG) and recovery 83.7 to 113.4% (O^6 -CMdG) or 92.1 to 122.6% (O^6 -MedG) of the actual adduct level.

dG Quantification by Liquid Chromatography. Quantitation of dG was carried out by reversed-phase HPLC with a diode array detector set to monitor absorbance at $\lambda = 254$ nm on a C18 Kinetex column, 2.1×150 mm, particle size 2.6 μm , pore size 100 \AA column (Phenomenex, Torrance, California) using 3% ACN in H_2O as mobile phase A and ACN as mobile phase B. Chromatographic separation was achieved by a gradient from 100% A to 88% A in 6 min at a flow rate of 0.2 mL/min. The injection volume was 20 μL . The retention times for nucleosides were the following: dC 3.5 min, dG 8.4 min, dT 9.2 min, and dA 10.6 min. A calibration curve for dG (0.1, 1, 10, 25, 50, and 100 μM) was analyzed. The amount of dG was then used to calculate the total number of nucleotides based on the assumption that the GC content is 40.9% in human DNA.⁴³

RESULTS

Stability of L-Azaserine at Varying pH and Biological Matrices. The hydrolysis of L-azaserine to yield L-serine and diazoacetate has been previously suggested as a basis for the formation of O^6 -CMdG (Figure 1B).¹⁷ However, this mechanism raises concern about the wide use of L-azaserine in cell-based studies and whether the compound is stable under the experimental conditions of in vitro toxicological assays. Therefore, we sought to characterize the stability of L-azaserine as a function of pH and in the presence of biological matrices. First, levels of L-azaserine and its hydrolysis product L-serine were measured in solutions ranging in pH from pH 2 to 11 at 25 $^\circ\text{C}$ over the course of 5 days. No decomposition was observed between pH 5.8 and 10.5, while at pH 2, L-azaserine was completely hydrolyzed to L-serine after 2 h (Figure S8). The acid-catalyzed hydrolysis was modeled as a pseudo-first-order reaction (Figure 2A), and the half-life ($t_{1/2}$) was calculated to be 0.4 h at pH 2, 0.7 h at pH 2.4, and 4.7 h at pH 3.4. Next, we assessed the stability of L-azaserine in the presence of cell culture medium, active whole cell lysates, and excess commercial porcine liver esterase. None of these biological matrices were active in catalyzing any conversion of L-azaserine at 37 $^\circ\text{C}$ from 10 min to 24 h (Figure S1). On the other hand, fluorescein diacetate, tested as a positive control at the same concentration, was completely hydrolyzed within a few minutes. Together, these data emphasize that L-azaserine resists hydrolysis under neutral physiological conditions in the presence of biological matrices and suggest

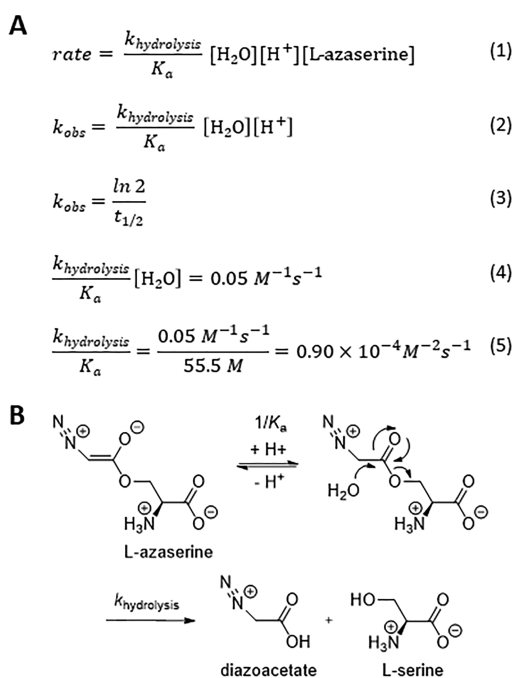


Figure 2. Acid-promoted hydrolysis of L-azaserine. (A) Rate law for hydrolysis of L-azaserine and relationship with observed values. (B) Proposed mechanism of acid-catalyzed hydrolysis of L-azaserine to L-serine.

against it being the initial step in the reaction of L-azaserine with DNA to give rise to O^6 -CMdG.

Evidence for O^6 -Ser-CMdG as the Intermediate in the Formation of O^6 -CMdG by L-Azaserine. Having established that L-azaserine does not undergo hydrolysis under physiologically relevant conditions, we considered whether under those conditions L-azaserine may directly react with dG to give rise to the direct adduct O^6 -Ser-CMdG, which then yields O^6 -CMdG upon spontaneous hydrolysis (Figure 1A). To gain support for this mechanism, we first explored whether O^6 -Ser-CMdG could be formed by reacting a 9-mer nucleotide with an excess L-azaserine in sodium phosphate buffer at 37 °C for 24 h. The crude reaction mixture was then analyzed by HPLC for the presence of newly formed oligonucleotide peaks (Figure S2), which were collected and further analyzed by electrospray ionization mass spectrometry. The electrospray mass spectrum and the fragmentation for the oligonucleotide that eluted at 22.0 min in the UV-chromatogram corresponded to the anticipated m/z values of the electrospray ionization mass for the O^6 -Ser-CMG-oligonucleotide (Figure S2), providing the first support for the direct reaction of L-azaserine with DNA. To allow robust and unambiguous characterization of the direct adduct, we decided to reduce the complexity of the reaction and allow dG to react with an excess of L-azaserine in tris-buffer at pH in the range of 7–11 for 0.5–24 h. The resulting reaction mixtures were analyzed for the presence of O^6 -Ser-CMdG, O^6 -CMdG, and O^6 -MedG by nanoLC-ESI-HRMS² in PRM mode. We monitored mass transitions accounting for neutral loss of deoxyribose followed by possible fragmentation of serine (Table 1).^{38–40} XICs of all reaction mixtures revealed the appearance of two peaks with the mass corresponding to O^6 -Ser-CMdG at a retention time of 17.9 and 18.1 min (Figure 3A). Their mass-fragments were the same, consistent with being two positional isomers of Ser-CMdG. Further, two peaks were detected with m/z corresponding to

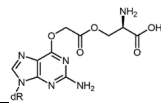
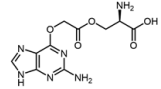
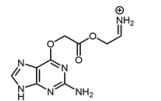
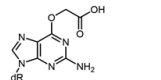
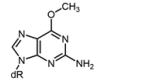
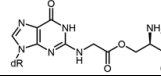
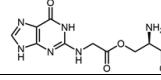
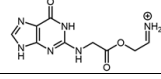
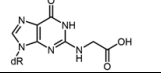
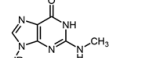
carboxymethylated dG with retention times close to the potential Ser-CMdG isomers, and one of them coeluted with the standard $^{15}\text{N}_5$ - O^6 -CMdG (18.35 min), thereby assigned as O^6 -CMdG. Similarly, two peaks were detected with m/z corresponding to isomers of MedG; one peak coeluted with an N^2 -MedG standard (18.01 min), while the second peak coeluted with the standard for O^6 -MedG (18.75 min). As a negative control, we performed the same reaction with potassium diazoacetate, and no peaks were detected corresponding to Ser-CMdG or fragments thereof, but the same two peaks for each carboxymethylation and methylation of dG as for the L-azaserine treated samples were observed (Figure 3B). None of the targeted m/z values were detected in control samples with any of the single reagents. These results suggest that L-azaserine reacts directly with dG, forming adducts that retain the serine moiety at the O^6 - and N^2 -positions.

O^6 -Ser-CMdG Decomposes to O^6 -CMdG. Having gained evidence for the formation of O^6 -Ser-CMdG intermediate in the reaction of dG with L-azaserine by mass spectrometry, we further characterized this novel structure and confirmed that it can be converted to O^6 -CMdG. Thus, by HPLC analysis, Ser-CMdG was observed in the reaction of dG with L-azaserine already after 30 min and remained detectable up to 120 h (18.7 min, m/z of 413, Figure S5A). The compound was purified by HPLC, and its ^1H NMR spectrum was consistent with Ser-CMdG due to the presence of three characteristic peaks at 5.07 (s, 1H, NH_2 -CH), 4.83–4.81 (m, 2H, $\text{O}-\text{CH}_2-\text{COO}$), and 3.93–3.84 ppm (m, 2H, $\text{O}-\text{CH}_2$), accounting for five additional Hs in addition to those present in dG (Figure S5C). The HRMS of the isolated peak revealed m/z 413.1411 (RT 17.56 min), corresponding to Ser-CMdG (Figure 3C). After isolation of Ser-CMdG by HPLC, analysis of the sample by mass spectrometry always revealed the presence of O^6 -CMdG, but not N^2 -CMdG, (Figure 3C), suggesting that the Ser-CMdG adduct eluting at retention time 17.56 is O^6 -Ser-CMdG.

Having established that O^6 -Ser-CMdG forms as a direct product of the reaction between dG and L-azaserine, we characterized further its aforementioned apparent hydrolysis to yield O^6 -CMdG. At pH 7.2, the disappearance of O^6 -Ser-CMdG (HPLC retention time 23 min) coincided with the appearance of O^6 -CMdG (HPLC retention time 43 min; Figure S6, identity confirmed by coelution with the authentic standard and consistent HRMS data (Figure 4)). We concluded that O^6 -Ser-CMdG is an intermediate in L-azaserine-induced O^6 -CMdG formation, thereby suggesting a possible mechanism for the formation of O^6 -CMdG in DNA under physiological conditions in which L-azaserine is stable.

Exposure of Cells to L-Azaserine and Quantification of Resulting Adducts. Having established that under neutral conditions direct alkylation of dG by L-azaserine occurs to form O^6 -Ser-CMdG that spontaneously hydrolyzes to yield O^6 -CMdG, we were interested in characterizing this process in cells and understanding the kinetic basis of adduct formation upon exposure to L-azaserine. Immortalized but normal diploid human colonic epithelial HCEC cells were employed as a model for adduct formation in healthy colon tissue.³⁵ HCEC cells express epithelial and stem cell markers and do not show mutations in genes known to be involved in colon cancer progression (*APC*, *KRAS*, *TP53*).⁴⁴ HCEC cells were exposed to L-azaserine for 0.5 to 120 h and at concentrations ranging from 125 to 1000 μM . Following DNA isolation and

Table 1. Targeted m/z with Proposed Structures for O^6 -Ser-CMdG and Transitions

Compound ^a	m/z MS ⁿ	Structure ^b	RT (min)	diazoacetate	L-azaserine	control	LC RT 18.7
O^6 -Ser-CMdG	413.1421 MS ¹		18.14	nd	413.1415	nd	413.1419
O^6 -Ser-CMG	297.0947 MS ²		18.14	nd	297.0941	nd	297.0937
O^6 -Ser-CMG – (H ₂ O+CO)	251.0893 MS ²		18.15	nd	251.0883	nd	251.0884
O^6 -CMdG	326.1096 MS ¹		18.37	326.1096	326.1094	nd	326.1099
¹⁵ N ₅ - O^6 -CMdG	331.0952 MS ¹		18.37	331.0944	331.0944	331.0944	331.0944
O^6 -MedG	282.1195 MS ¹		18.84	282.1196	282.1187	nd	282.1195
D ₃ - O^6 -MedG	285.1391 MS ¹		18.84	285.1383	285.1383	285.1383	285.1383
N^2 -Ser-CMdG	413.1421 MS ¹		17.91	nd	413.1418	nd	nd
N^2 -Ser-CMG	297.0947 MS ²		17.91	nd	297.0948	nd	nd
N^2 -Ser-CMG – (H ₂ O+CO)	251.0893 MS ²		17.89	nd	251.0882	nd	nd
N^2 -CMdG	326.1096 MS ¹		18.03	326.1095	326.1095	nd	nd
N^2 -MedG	282.1195 MS ¹		18.00	282.1195	282.1197	nd	nd

^a O^6 -substitution was confirmed by isotopically labeled O^6 -CMdG and O^6 -MedG standards. N^2 -coordination is confirmed by N^2 -MedG standard. ^bStructures and m/z of O^6 -CMdG and O^6 -MedG as hydrolysis products are included. Detected structures are indicated for diazoacetate, L-azaserine, and control samples from reaction mixture with dG and for the isolated compound by reversed-phase liquid chromatography (LC RT 18.7 min). nd = not detectable.

hydrolysis, products O^6 -CMdG and O^6 -MedG were detected, but no O^6 -Ser-CMdG intermediate in cells, either because levels were too low or because it is not formed in cells. While inconclusive regarding whether the chemical mechanism established herein is the same as what occurs in cells, the fact that we could not detect it was not surprising, given our observation of the high instability of the serine intermediate on the nucleotide level, and the procedure required to digest genomic DNA for analysis of modified nucleosides from cells. Despite not observing the transient intermediate in samples obtained from cells, in order to characterize overall rates of DNA damage induced by L-azaserine in cells, we validated the nanoLC-ESI-HRMS² method for the concomitant quantification of O^6 -CMdG and O^6 -MedG in cells with a stable isotope dilution method that accounts for losses during sample

preparation and ionization and allows for accurate quantification of the analyte based on the ratio of its signal area to that of labeled internal standard. PRM was applied for the mass transitions corresponding to a neutral loss of deoxyribose (dR) from the protonated analytes: O^6 -CMdG and O^6 -MedG, and their isotopically labeled internal standards ¹⁵N₅- O^6 -CMdG and D₃- O^6 -MedG.

O^6 -CMdG and O^6 -MedG Levels in HCEC Cells. The robust nanoLC-ESI-HRMS² approach for simultaneously quantifying O^6 -CMdG and O^6 -MedG enabled the measurement of L-azaserine-induced adducts in HCEC cells in a dose- and time-dependent manner. The level of both adducts increased linearly with L-azaserine concentration (0–1000 μ M, 4 h exposure), with maximum adduct levels of 32.8 ± 7.8 O^6 -CMdG and 4.3 ± 0.9 O^6 -MedG lesions/ 10^7 nucleotides

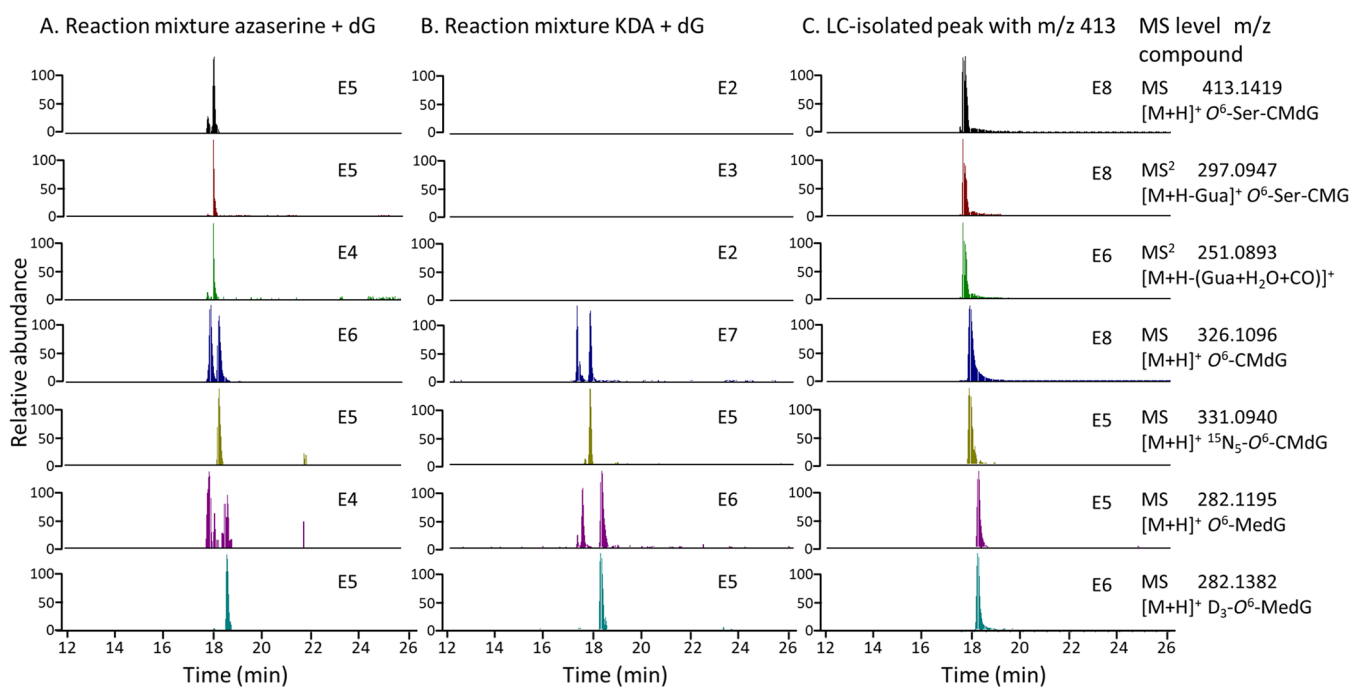


Figure 3. Representative chromatograms for the reaction of dG with L-azaserine or potassium diazoacetate analyzed by nanoLC-ESI-HRMS². (A, B) 5 μ M dG was reacted with 5 mM L-azaserine (A) or potassium diazoacetate (B) as control in 10 mM tris-buffer at pH 7, followed by SPE and nanoLC-ESI-HRMS². (C) 4 mM dG was reacted with 25 mM L-azaserine in 0.1 M sodium phosphate buffer and peak with m/z 413 isolated by LC, concentrated, and analyzed by nanoLC-ESI-HRMS². XICs represent parent mass for O^6 -Ser-CMdg and two fragmentations, followed by O^6 -CMdg, $^{15}N_5$ - O^6 -CMdg as internal standard, O^6 -MedG and D_3 - O^6 -MedG as internal standard. The sample represented in (C) was analyzed on a new column, explaining the shift in absolute retention time, while the Δ between O^6 -Ser-CMdg and O^6 -CMdg was equal.

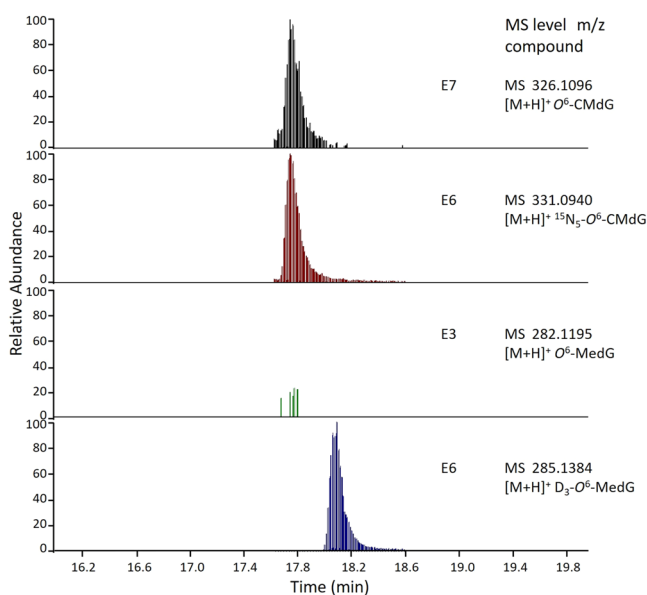


Figure 4. NanoLC-ESI-HRMS² chromatogram for the decomposition product of O^6 -Ser-CMdg. Decomposition product was isolated by reversed-phase LC and identified as O^6 -CMdg by nanoLC-ESI-HRMS². No methylated dG could be detected. The m/z values are determined experimentally.

(Figure 5, for representative MS2 spectra, see Figures S9 and S10). Levels of O^6 -CMdg were low compared to O^6 -MedG, as reported previously.^{17,27} We also detected O^6 -CMdg in unexposed control samples but at levels below LOQ, while 0.7 ± 1.3 O^6 -MedG adducts/ 10^7 nucleotides could be quantified in unexposed control samples. Endogenous O^6 -

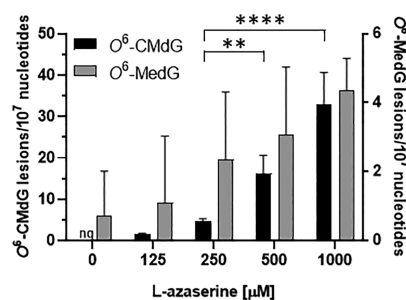


Figure 5. Dose-dependent formation of O^6 -CMdg and O^6 -MedG in HCEC cells. Cells were exposed for 4 h to 0, 125, 250, 500, or 1000 μ M L-azaserine, and extracted DNA was analyzed for O^6 -CMdg and O^6 -MedG by nanoLC-ESI-HRMS². Adduct levels are expressed as lesions/ 10^7 nucleotides (mean \pm SD, $n = 3$). P -values were calculated with one-way ANOVA and Tukey's multiple comparison's test, ** $p < 0.005$, **** $p < 0.0001$.

CMdg was previously reported in human colorectal cells (HCT-166) and in XPA-deficient human fibroblast cells, and O^6 -MedG is very well-known to be formed endogenously.^{27,45}

Having established the dose-dependent formation of O^6 -CMdg and O^6 -MedG after 4 h exposure to L-azaserine, we were interested in the temporal profiles of the DNA adducts. Therefore, we exposed HCEC cells to 500 μ M L-azaserine (EC₄₀ after 120 h, Figure S11) for various durations (0.5, 4, 10, 24, 48, 72, 96, 120 h). After 0.5 h, adduct levels were below the LOQ for O^6 -CMdg and O^6 -MedG. O^6 -CMdg levels increased during the first 48 h to a maximum adduct level of 116 ± 21 O^6 -CMdg lesions/ 10^7 nucleotides (Figure 6) and plateaued after, displaying no changes in adduct level for the remaining 3 days. Also, O^6 -MedG levels reached a maximum value after 48 h; however, we could not establish a time-dependent

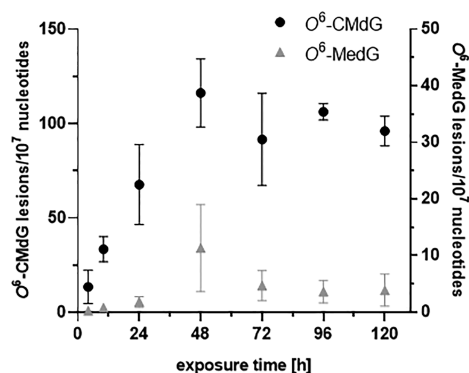


Figure 6. Time-dependent formation of O^6 -CMdG and O^6 -MedG in HCEC cells. Cells were exposed to 500 μ M *L*-azaserine, and DNA was extracted after 0.5, 4, 10, 24, 48, 72, 96, and 120 h and further analyzed for O^6 -CMdG and O^6 -MedG levels by nanoLC-ESI-HRMS². Adduct levels are expressed as lesions/10⁷ nucleotides (mean \pm SD, $n = 3$).

relationship due to the overall low level of O^6 -MedG adducts formed in HCEC exposed to 500 μ M *L*-azaserine.

DISCUSSION

NOCs are well-known carcinogens linked to diet and lifestyle. The formation of the pro-mutagenic DNA adducts O^6 -CMdG and O^6 -MedG by NOCs is well established;^{8,10,16,17,27} however, understanding of the chemical mechanism of NOC-induced O^6 -CMdG formation and factors that influence their biological consequences is limited. It has been hypothesized that the release of diazoacetate from NOCs and analogs is responsible for the carboxymethylation and methylation of DNA. However, if the reactive intermediate is the same for various NOCs, such as *N*-(*N*-acetyl-*L*-prolyl)-*N*-nitrosoglycine (APNG) and *N*-nitrosoglycocholic acid (NOGC), and for the reactive intermediates *L*-azaserine and diazoacetate, it remains unclear why they all result in different ratios of O^6 -CMdG to O^6 -MedG.^{17,46} Further, the carboxymethylating decomposition products of *N*-nitroso bile acid conjugates have not been recovered quantitatively.⁴⁷ The lack of characterization of the metabolism of NOCs and of reactive intermediates raises the question of what are the mechanisms of carboxymethylation and methylation of DNA by NOCs, including the possibility of several pathways and intermediates.

Hydrolysis of *L*-azaserine to *L*-serine and diazoacetate has been suggested earlier by Harrison et al.,¹⁷ and decomposition to diazoacetate as the intermediate in O^6 -CMdG formation has been demonstrated for *N*-nitroso-glycine under physiological conditions.¹¹ However, in this study, we demonstrated that the carboxymethylating agent *L*-azaserine undergoes hydrolysis to *L*-serine only under acidic conditions and that under physiologically relevant conditions in the presence of biological matrices, *L*-azaserine is stable. The half-life of *L*-azaserine was 0.4 h at pH 2, and its stability increased with increasing pH, consistent with an acid-catalyzed hydrolysis mechanism. Protonation of the diazocarbonyl moiety, possibly at the carbon bound to both the diazo and carbonyl groups, is expected to promote hydrolysis of the ester and release *L*-serine (Figure 2B). On the basis of the pH dependence of the protonation/hydrolysis rates and having derived k_{obs} for each pH value (Table S2), we estimated the ratio $k_{\text{hydrolysis}}/K_a$ to be $0.90 \times 10^{-4} \text{ M}^{-1} \text{ s}^{-1}$ (Figure 2A, eq 5). The pK_a of the protonated *L*-azaserine (Figure 2A) could not be extracted,

while similar diazo compounds such as diazomethane have a pK_a of 10, such a high value would be inconsistent with the pH-stability profile of *L*-azaserine.⁴⁸ The observation of acid-promoted decomposition of *L*-azaserine is consistent with a previous report of loss of antibiotic activity and N_2 formation at pH 2 for *L*-azaserine.⁴⁹ Indeed, α -diazo compounds are acid labile, resulting in formation of reactive alkenium ions and loss of N_2 .⁵⁰ Acid-promoted decomposition was also demonstrated for diazo peptides and *N*-nitroso peptides, while under physiological conditions they are stable.^{51,52} Finally, under neutral conditions, diazoacetate was demonstrated to be an intermediate of *N*-nitroso-glycine-induced O^6 -CMdG and O^6 -MedG formation, potentially via formation of carboxymethyl-diazonium ion and diazomethane, whereas, to our knowledge, the decomposition of NOCs with more stabilized α -diazocarboxy-groups,⁵³ for example, diazo peptides, has not been characterized under physiological conditions.¹¹

Based on the lack of evidence for the decomposition of *L*-azaserine at neutral pH in the presence of active whole cell lysates, we hypothesized that *L*-azaserine reacts directly with DNA under physiological conditions. The formation of a direct reaction product Ser-CMdG from *L*-azaserine has been previously proposed, but to our knowledge was never investigated.^{17,54} Data from reactions with oligonucleotides and with dG revealed the existence of the intermediate O^6 -Ser-CMdG (Figure 1). We did not observe any correlation of levels of the direct adduct with time or pH; however, the amount that could be obtained from oligonucleotides was extremely small and transient on the nucleotide level, making any clear kinetic conclusions elusive. The other regioisomer observed was assigned as N^2 -SerCMdG. On the basis of peak area, and approximating the same recovery and ionization behavior, it appears to be on average about 3 times less abundant than O^6 -SerCMdG. However, for CMdG and MedG adducts, the $N^2:O^6$ ratio was 1.3 and 1.1, respectively. Interestingly, for the reaction with diazoacetate, the $N^2:O^6$ ratio was 2 for O^6 -CMdG and 0.7 for O^6 -MedG, suggesting the adducts were formed via a different chemical mechanism. Diazo compounds with stabilizing electron withdrawing groups are a useful tool in the modification and detection of biomolecules,⁵³ as demonstrated by the use of ethyldiazoacetate in carboxylation of dG.³⁶ Next to the O^6 - position, N^7 , N^3 , N^2 , and N^1 represent nucleophilic sites in dG that are susceptible to modification by electrophilic reagents.⁵⁵ N^7 -CMG and N^7 -MeG have been detected after in vitro NOCs exposure, however, these readily depurinate.^{25,54} Further, two methylated-dG adducts with modification other than at the O^6 -position were detected previously after exposure of ctDNA to potassium diazoacetate, and one carboxymethylated-dG adduct other than O^6 was present in colon tumor biopsy samples analyzed by a HRMS² approach for establishing a diet-related DNA adduct database.⁸

While evidence for the direct serine adduct could not be gained from samples of genomic DNA from *L*-azaserine-exposed cells, we characterized the formation and persistence of O^6 -CMdG and O^6 -MedG as a function of *L*-azaserine dose and time of exposure with a robust and sensitive nanoLC-ESI-HRMS² PRM method validated for analysis of cell samples. To our knowledge, this is the first HRMS approach for the absolute quantification of O^6 -MedG and O^6 -CMdG in biological samples using stable isotope-labeled internal standards for accurate quantification of both adducts. A few methods involving triple quadrupole or ion traps as mass analyzer exist for the detection and quantification of O^6 -

CM(d)G in biological samples,⁵⁶ also in combination with O⁶-Me(d)G.^{10,27} A HRMS methodology targeting O⁶-MeG and O⁶-CMG and other targeted and untargeted DNA adducts was successfully applied to colon biopsy samples to establish a diet-related DNA adducts database and to compare the DNA adduct profile from white vs red meat in gastrointestinal digestion samples.^{8,15} O⁶-MedG was further one of the targeted adducts in a reported adductomic approach for nitrosamine-induced DNA adducts.⁵⁷ Validation of our nanoLC-ESI-HRMS² approach revealed LOQs in matrix were in the low amol range and comparable to LOQs previously reported for pure standards on nanoLC-ESI-MS^{3,27} and improved compared to a HRMS method targeting four adducts in biological matrix.⁸ Applying our methodology to HCEC cell exposed to L-azaserine, we found a linear response between L-azaserine dose and O⁶-CMdG and O⁶-MedG adduct levels in HCEC cells (Figure 5). Both adducts were present in unexposed control samples, though not quantifiable for O⁶-CMdG and below one O⁶-MedG adduct/10⁷ nucleotides. We measured maximal O⁶-CMdG adduct levels in cells after 48 h of exposure, followed by a steady level up to 120 h (Figure 6). The O⁶-MedG profile showed a similar trend, but the adduct levels were too low for statistical analysis. The low O⁶-MedG levels observed are consistent with the more potent O⁶-CMdG formation by L-azaserine.^{16,17} Additionally, low levels of O⁶-MedG measured in cells might be due to efficient repair of O⁶-MedG by O⁶-methylguanine DNA methyl transferase.⁵⁸ In a previous study, a maximum N⁷-MeG adduct level was achieved also after 48 h exposure to NDMA, however, in a process requiring metabolic activation by CYP enzymes.⁵⁹ Adduct levels were on the same order of magnitude as previously reported for colorectal cancer cells exposed to L-azaserine,²⁷ which was more potent in inducing O⁶-CMdG.²⁷ Endogenous O⁶-CMdG and O⁶-MedG formation has been reported previously and is likely due to the endogenous formation of s-adenosylmethionine and NOCs,^{27,60–62} which account for 45–75% of the total human NOC exposure.^{19,63}

CONCLUSION

In this study, we characterized the chemical basis of L-azaserine-induced O⁶-CMdG formation. We identified two mechanisms, occurring under acidic and physiological conditions, respectively, by which L-azaserine converts into reactive intermediates and induces O⁶-CMdG. Our findings have implications for endogenously formed NOCs that do not breakdown to diazoacetate under physiological conditions but can form DNA adducts via nucleophilic attack. We established a highly sensitive nanoLC-ESI-HRMS² methodology and measured a linear dose-response relationship for O⁶-CMdG lesions in cells after exposure to L-azaserine. The knowledge of L-azaserine-induced DNA adduct formation has important implications to understand O⁶-CMdG formation and accumulation in cells and to study its biological consequences. Overall, this work provides fundamental chemical insight concerning the basis of how L-azaserine may give rise to DNA damage and supports its use as a chemical probe in NOC-induced carcinogenesis research, particularly concerning the identification of factors that mitigate adverse effects of O⁶-CMdG.

ASSOCIATED CONTENT

Supporting Information

The Supporting Information is available free of charge at <https://pubs.acs.org/doi/10.1021/acs.chemrestox.0c00471>.

Figure S1: Stability of L-azaserine in the presence of biological matrices. Figure S2: Formation of O⁶-Ser-CMG in an oligonucleotide. Figures S3–S6: Compound characterizations. Figure S7: Analytical calibration curves. Figure S8: Acid-catalyzed hydrolysis of L-azaserine. Figure S9: Cell viability data. Figures S10 and S11: Representative MS² data from analysis of genomic DNA samples. Table S1: L-Azaserine decomposition rates. Table S2: Precision and accuracy of adduct analysis method (PDF)

AUTHOR INFORMATION

Corresponding Author

Shana J. Sturla – Department of Health Science and Technology, ETH Zurich, 8092 Zurich, Switzerland; orcid.org/0000-0001-6808-5950; Email: sturlas@ethz.ch

Authors

Susanne M. Geisen – Department of Health Science and Technology, ETH Zurich, 8092 Zurich, Switzerland; orcid.org/0000-0002-9394-0274

Claudia M. N. Aloisi – Department of Health Science and Technology, ETH Zurich, 8092 Zurich, Switzerland; orcid.org/0000-0002-2279-7757

Sabrina M. Huber – Department of Health Science and Technology, ETH Zurich, 8092 Zurich, Switzerland; orcid.org/0000-0001-9204-5537

Emma S. Sandell – Department of Health Science and Technology, ETH Zurich, 8092 Zurich, Switzerland; orcid.org/0000-0002-8066-5293

Nora A. Escher – Department of Health Science and Technology, ETH Zurich, 8092 Zurich, Switzerland

Complete contact information is available at: <https://pubs.acs.org/doi/10.1021/acs.chemrestox.0c00471>

Funding

This work was supported by the Swiss National Science Foundation (185020, 186332) and the Swiss Cancer Research Foundation (KFS-4443-02-2018-R).

Notes

The authors declare no competing financial interest.

ACKNOWLEDGMENTS

The authors wish to thank the staff of the Functional Genomics Center Zurich (FGCZ) for providing nanoLC-ESI-HRMS² instrumentation and technical support, namely Dr. Bernd Roschitzki, Dr. Peter Gehrig, Dr. Serena di Palma, Dr. Endre Laczko, and Laura Kunz. We also thank Dr. Hailey Gahlon for scientific advice and Jonne van Dijk for her technical support in sample preparation.

REFERENCES

- (1) Bouvard, V.; Loomis, D.; Guyton, K. Z.; Grosse, Y.; Ghissassi, F. E.; Benbrahim-Tallaa, L.; Guha, N.; Mattock, H.; and Straif, K. (2015) Carcinogenicity of consumption of red and processed meat. *Lancet Oncol.* 16 (16), 1599–1600.
- (2) Aloisi, C. M. N., Sandell, E. S., and Sturla, S. J. (2021) A chemical link between meat consumption and colorectal cancer development? *Chem. Res. Toxicol.* 34, 12–23.
- (3) Turesky, R. J. (2018) Mechanistic Evidence for Red Meat and Processed Meat Intake and Cancer Risk: A Follow-up on the

International Agency for Research on Cancer Evaluation of 2015. *Chimia* 72 (10), 718–724.

(4) Loechler, E. L., Green, C. L., and Essigmann, J. M. (1984) In vivo mutagenesis by O^6 -methylguanine built into a unique site in a viral genome. *Proc. Natl. Acad. Sci. U. S. A.* 81 (20), 6271–6275.

(5) Pauly, G. T., and Moschel, R. C. (2001) Mutagenesis by O^6 -Methyl-, O^6 -Ethyl-, and O^6 -Benzylguanine and O^4 -Methylthymine in Human Cells: Effects of O^6 -Alkylguanine-DNA Alkyltransferase and Mismatch Repair. *Chem. Res. Toxicol.* 14 (7), 894–900.

(6) Hall, C. N., Badawi, A. F., O'Connor, P. J., and Saffhill, R. (1991) The detection of alkylation damage in the DNA of human gastrointestinal tissues. *Br. J. Cancer* 64 (1), 59–63.

(7) O^6 -methylguanine in blood leucocyte DNA: an association with the geographic prevalence of gastric cancer and with low levels of serum pepsinogen A, a marker of severe chronic atrophic gastritis. *Carcinogenesis* 1994, 15 (9), 1815–20.

(8) Hemeryck, L. Y., Declodet, A. I., Vanden Bussche, J., Geboes, K. P., and Vanhaecke, L. (2015) High resolution mass spectrometry based profiling of diet-related deoxyribonucleic acid adducts. *Anal. Chim. Acta* 892, 123–131.

(9) Povey, A. C., Hall, C. N., Badawi, A. F., Cooper, D. P., and O'Connor, P. J. (2000) Elevated levels of the pro-carcinogenic adduct, O^6 -methylguanine, in normal DNA from the cancer prone regions of the large bowel. *Gut* 47 (3), 362–365.

(10) Vanden Bussche, J., Moore, S. A., Pasmans, F., Kuhnle, G. G. C., and Vanhaecke, L. (2012) An approach based on ultra-high pressure liquid chromatography–tandem mass spectrometry to quantify O^6 -methyl and O^6 -carboxymethylguanine DNA adducts in intestinal cell lines. *Journal of Chromatography A* 1257, 25–33.

(11) Cupid, B. C., Zeng, Z., Singh, R., and Shuker, D. E. G. (2004) Detection of O^6 -Carboxymethyl-2'-deoxyguanosine in DNA Following Reaction of Nitric Oxide with Glycine and in Human Blood DNA Using a Quantitative Immunoblot Assay. *Chem. Res. Toxicol.* 17 (3), 294–300.

(12) Lewin, M. H., Bailey, N., Bandaletova, T., Bowman, R., Cross, A. J., Pollock, J., Shuker, D. E. G., and Bingham, S. A. (2006) Red Meat Enhances the Colonic Formation of the DNA Adduct O^6 -Carboxymethyl Guanine: Implications for Colorectal Cancer Risk. *Cancer Res.* 66 (3), 1859–1865.

(13) Bussche, J. V., Hemeryck, L. Y., Van Hecke, T., Kuhnle, G. G. C., Pasmans, F., Moore, S. A., Van de Wiele, T., De Smet, S., and Vanhaecke, L. (2014) O^6 -carboxymethylguanine DNA adduct formation and lipid peroxidation upon in vitro gastrointestinal digestion of haem-rich meat. *Mol. Nutr. Food Res.* 58 (9), 1883–1896.

(14) Hemeryck, L. Y., Rombouts, C., Hecke, T. V., Van Meulebroek, L., Bussche, J. V., De Smet, S., and Vanhaecke, L. (2016) In vitro DNA adduct profiling to mechanistically link red meat consumption to colon cancer promotion. *Toxicol. Res. (Cambridge, U. K.)* 5 (5), 1346–1358.

(15) Hemeryck, L. Y., Rombouts, C., De Paep, E., and Vanhaecke, L. (2018) DNA adduct profiling of in vitro colonic meat digests to map red vs. white meat genotoxicity. *Food Chem. Toxicol.* 115, 73–87.

(16) Harrison, K. L., Fairhurst, N., Challis, B. C., and Shuker, D. E. G. (1997) Synthesis, Characterization, and Immunochemical Detection of O^6 -(Carboxymethyl)-2'-deoxyguanosine: A DNA Adduct Formed by Nitrosated Glycine Derivatives. *Chem. Res. Toxicol.* 10 (6), 652–659.

(17) Harrison, K. L., Jukes, R., Cooper, D. P., and Shuker, D. E. G. (1999) Detection of Concomitant Formation of O^6 -Carboxymethyl- and O^6 -Methyl-2'-deoxyguanosine in DNA Exposed to Nitrosated Glycine Derivatives Using a Combined Immunoaffinity/HPLC Method. *Chem. Res. Toxicol.* 12 (1), 106–111.

(18) Stuff, J. E., Goh, E. T., Barrera, S. L., Bondy, M. L., and Forman, M. R. (2009) Construction of an N-nitroso database for assessing dietary intake. *J. Food Compos. Anal.* 22, S42–S47.

(19) Mirvish, S. S. (1995) Role of N-nitroso compounds (NOC) and N-nitrosation in etiology of gastric, esophageal, nasopharyngeal and bladder cancer and contribution to cancer of known exposures to NOC. *Cancer Lett.* 93 (1), 17–48.

(20) Wu, J., Wang, P., Li, L., Williams, N. L., Ji, D., Zahurancik, W. J., You, C., Wang, J., Suo, Z., and Wang, Y. (2017) Replication studies of carboxymethylated DNA lesions in human cells. *Nucleic Acids Res.* 45 (12), 7276–7284.

(21) Ráz, M. H., Dexter, H. R., Millington, C. L., van Loon, B., Williams, D. M., and Sturla, S. J. (2016) Bypass of Mutagenic O^6 -Carboxymethylguanine DNA Adducts by Human γ - and β -Family Polymerases. *Chem. Res. Toxicol.* 29 (9), 1493–503.

(22) Gottschalg, E., Scott, G. B., Burns, P. A., and Shuker, D. E. (2006) Potassium diazoacetate-induced p53 mutations in vitro in relation to formation of O^6 -carboxymethyl- and O^6 -methyl-2'-deoxyguanosine DNA adducts: relevance for gastrointestinal cancer. *Carcinogenesis* 28 (2), 356–62.

(23) Andreyev, H. J., Norman, A. R., Cunningham, D., Oates, J., Dix, B. R., Iacopetta, B. J., Young, J., Walsh, T., Ward, R., Hawkins, N., Beranek, M., Jandik, P., Benamouzig, R., Jullian, E., Laurent-Puig, P., Olschwang, S., Muller, O., Hoffmann, I., Rabes, H. M., Zietz, C., Troungos, C., Valavanis, C., Yuen, S. T., Ho, J. W., Croke, C. T., O'Donoghue, D. P., Giaretti, W., Rapallo, A., Russo, A., Bazan, V., Tanaka, M., Omura, K., Azuma, T., Ohkusa, T., Fujimori, T., Ono, Y., Pauly, M., Faber, C., Glaesener, R., de Goeij, A. F., Arends, J. W., Andersen, S. N., Lövig, T., Breivik, J., Gaudernack, G., Clausen, O. P., De Angelis, P. D., Meling, G. I., Rognum, T. O., Smith, R., Goh, H. S., Font, A., Rosell, R., Sun, X. F., Zhang, H., Benhattar, J., Losi, L., Lee, J. Q., Wang, S. T., Clarke, P. A., Bell, S., Quirke, P., Bubb, V. J., Piris, J., Cruickshank, N. R., Morton, D., Fox, J. C., Al-Mulla, F., Lees, N., Hall, C. N., Snary, D., Wilkinson, K., Dillon, D., Costa, J., Pricolo, V. E., Finkelstein, S. D., Thebo, J. S., Senagore, A. J., Halter, S. A., Wadler, S., Malik, S., Krtolica, K., and Urošević, N. (2001) Kirsten ras mutations in patients with colorectal cancer: the 'RASCAL II' study. *Br. J. Cancer* 85 (5), 692–696.

(24) Wang, J., and Wang, Y. (2011) Carboxymethylation of DNA Induced by N-Nitroso Compounds and Its Biological Implications. *Advances in Molecular Toxicology* 5, 219–243.

(25) Shuker, D. E. G., and Margison, G. P. (1997) Nitrosated Glycine Derivatives as a Potential Source of O^6 -Methylguanine in DNA. *Cancer Res.* 57 (3), 366–369.

(26) O'Driscoll, M., Macpherson, P., Xu, Y.-Z., and Karran, P. (1999) The cytotoxicity of DNA carboxymethylation and methylation by the model carboxymethylating agent azaserine in human cells. *Carcinogenesis* 20 (9), 1855–1862.

(27) Yu, Y., Wang, J., Wang, P., and Wang, Y. (2016) Quantification of Azaserine-Induced Carboxymethylated and Methylated DNA Lesions in Cells by Nanoflow Liquid Chromatography-Nanoelectrospray Ionization Tandem Mass Spectrometry Coupled with the Stable Isotope-Dilution Method. *Anal. Chem.* 88 (16), 8036–8042.

(28) Wang, J., and Wang, Y. (2009) Chemical synthesis of oligodeoxyribonucleotides containing N^3 - and O^4 -carboxymethylthymidine and their formation in DNA. *Nucleic Acids Res.* 37 (2), 336–45.

(29) Stock, C. C., Reilly, H. C., Buckley, S. M., Clarke, D. A., and Rhodas, C. P. (1954) Azaserine, A New Tumour-Inhibitory Substance: Studies with Crocker Mouse Sarcoma 180. *Nature* 173 (4393), 71–72.

(30) Longnecker, D. S., and Curphey, T. J. (1975) Adenocarcinoma of the Pancreas in Azaserine-treated Rats. *Cancer Res.* 35 (8), 2249–2257.

(31) Lilja, H. S., Hyde, E., Longnecker, D. S., and Yager, J. D. (1977) DNA Damage and Repair in Rat Tissues following Administration of Azaserine. *Cancer Res.* 37 (11), 3925–3931.

(32) Rosenkrantz, H., Sprague, R., Schaeppi, U., Pittillo, R. T., Cooney, D. A., and Davis, R. D. (1972) The stoichiometric fate of azaserine metabolized in vitro by tissues from azaserine-treated dogs and mice. *Toxicol. Appl. Pharmacol.* 22 (4), 607–620.

(33) Jacquez, J. A., and Sherman, J. H. (1962) Enzymatic Degradation of Azaserine. *Cancer Res.* 22 (1), 56–61.

- (34) Longenecker, J. B., and Snell, E. E. (1957) Pyridoxal and metal ion catalysis of alpha, beta elimination reactions of serine-3-phosphate and related compounds. *J. Biol. Chem.* 225 (1), 409–418.
- (35) Zhang, L., Kim, S., Jia, G., Buhmeida, A., Dallol, A., Wright, W. E., Fornace, A. J., Al-Qahtani, M., and Shay, J. W. (2015) Exome Sequencing of Normal and Isogenic Transformed Human Colonic Epithelial Cells (HCECs) Reveals Novel Genes Potentially Involved in the Early Stages of Colorectal Tumorigenesis. *BMC Genomics* 16 (1), S8.
- (36) Geigle, S. N., Wyss, L. A., Sturla, S. J., and Gillingham, D. G. (2017) Copper carbenes alkylate guanine chemoselectively through a substrate directed reaction. *Chemical Science* 8 (1), 499–506.
- (37) Reza, F., Bhaswati, G., Pei-Pei, K., Gaffney, B. L., and Jones, R. A. (1990) Synthesis of 6-substituted 2'-deoxyguanosine derivatives using trifluoroacetic anhydride in pyridine. *Tetrahedron Lett.* 31 (3), 319–321.
- (38) Zhang, P., Chan, W., Ang, I. L., Wei, R., Lam, M. M. T., Lei, K. M. K., and Poon, T. C. W. (2019) Revisiting Fragmentation Reactions of Protonated α -Amino Acids by High-Resolution Electrospray Ionization Tandem Mass Spectrometry with Collision-Induced Dissociation. *Sci. Rep.* 9 (1), 6453.
- (39) Rogalewicz, F., Hoppilliard, Y., and Ohanessian, G. (2000) Fragmentation mechanisms of α -amino acids protonated under electrospray ionization: a collisional activation and ab initio theoretical study. *Int. J. Mass Spectrom.* 195–196, 565–590.
- (40) Piraud, M., Vianey-Saban, C., Petritis, K., Elfakir, C., Steghens, J.-P., Morla, A., and Bouchu, D. (2003) ESI-MS/MS analysis of underivatized amino acids: a new tool for the diagnosis of inherited disorders of amino acid metabolism. Fragmentation study of 79 molecules of biological interest in positive and negative ionisation mode. *Rapid Commun. Mass Spectrom.* 17 (12), 1297–1311.
- (41) MycoAlert Assay Control Set, Lonza online protocol, https://bioscience.lonza.com/lonza_bs/CH/en/download/product/asset/27672 (accessed 2021-5-25).
- (42) CellTiter-Glo Luminescent Cell Viability Assay, Promega. <https://ch.promega.com/-/media/files/resources/protocols/technical-bulletins/0/celltiter-glo-luminescent-cell-viability-assay-protocol.pdf> (accessed 2021-5-25).
- (43) Piovesan, A., Pelleri, M. C., Antonaros, F., Strippoli, P., Caracausi, M., and Vitale, L. (2019) On the length, weight and GC content of the human genome. *BMC Res. Notes* 12 (1), 106.
- (44) Roig, A. I., Eskiocak, U., Hight, S. K., Kim, S. B., Delgado, O., Souza, R. F., Spechler, S. J., Wright, W. E., and Shay, J. W. (2010) Immortalized Epithelial Cells Derived From Human Colon Biopsies Express Stem Cell Markers and Differentiate In Vitro. *Gastroenterology* 138 (3), 1012–1021.e5.
- (45) Nakamura, J., Mutlu, E., Sharma, V., Collins, L., Bodnar, W., Yu, R., Lai, Y., Moeller, B., Lu, K., and Swenberg, J. (2014) The endogenous exposome. *DNA Repair* 19, 3–13.
- (46) Shuker, D. E. G., and Margison, G. P. (1997) Nitrosated Glycine Derivatives as a Potential Source of O^6 -Methylguanine in DNA. *Cancer Res.* 57 (3), 366–369.
- (47) Shuker, D. E. G., Tannenbaum, S. R., and Wishnok, J. S. (1981) N-Nitroso bile acid conjugates. I. Synthesis, chemical reactivity and mutagenic activity. *J. Org. Chem.* 46 (10), 2092–2096.
- (48) McGarrity, J. F., and Smyth, T. (1980) Hydrolysis of diazomethane-kinetics and mechanism. *J. Am. Chem. Soc.* 102 (24), 7303–7308.
- (49) Bartz, Q. R., Elder, C. C., Frohardt, R. P., Fusari, S. A., Haskell, T. H., Johannessen, D. W., and Ryder, A. (1954) Isolation and characterization of azaserine. *Nature* 173 (4393), 72–73.
- (50) Reglitz, M. (2012) *Diazo Compounds: Properties and Synthesis*, Academic Press, Orlando, FL.
- (51) Challis, B. C. (1989) Chemistry and biology of nitrosated peptides. *Cancer Surv.* 8 (2), 363–384.
- (52) Challis, B. C., Hopkins, A. R., Milligan, J. R., Mitchell, R. C., and Massey, R. C. (1984) Nitrosation of peptides. *IARC Sci. Publ.* 57, 61–70.
- (53) Mix, K. A., Aronoff, M. R., and Raines, R. T. (2016) Diazo Compounds: Versatile Tools for Chemical Biology. *ACS Chem. Biol.* 11 (12), 3233–3244.
- (54) Zurlo, J., Curphey, T. J., Hiley, R., and Longnecker, D. S. (1982) Identification of 7-Carboxymethylguanine in DNA from Pancreatic Acinar Cells Exposed to Azaserine. *Cancer Res.* 42 (4), 1286–1288.
- (55) Liu, S., and Wang, Y. (2015) Mass spectrometry for the assessment of the occurrence and biological consequences of DNA adducts. *Chem. Soc. Rev.* 44 (21), 7829–7854.
- (56) Da Pieve, C., Sahgal, N., Moore, S. A., and Velasco-Garcia, M. N. (2013) Development of a liquid chromatography/tandem mass spectrometry method to investigate the presence of biomarkers of DNA damage in urine related to red meat consumption and risk of colorectal cancer. *Rapid Commun. Mass Spectrom.* 27 (21), 2493–503.
- (57) Balbo, S., Hecht, S. S., Upadhyaya, P., and Villalta, P. W. (2014) Application of a High-Resolution Mass-Spectrometry-Based DNA Adductomics Approach for Identification of DNA Adducts in Complex Mixtures. *Anal. Chem.* 86 (3), 1744–1752.
- (58) Pegg, A. E. (2000) Repair of $O(6)$ -alkylguanine by alkyltransferases. *Mutat. Res., Rev. Mutat. Res.* 462 (2–3), 83–100.
- (59) Lin, H.-I., and Hollenberg, P. F. (2001) N-Nitrosodimethylamine-Mediated Formation of Oxidized and Methylated DNA Bases in a Cytochrome P450 2E1 Expressing Cell Line. *Chem. Res. Toxicol.* 14 (5), 562–566.
- (60) Sharma, V., Collins, L. B., Clement, J. M., Zhang, Z., Nakamura, J., and Swenberg, J. A. (2014) Molecular Dosimetry of Endogenous and Exogenous $O(6)$ -Methyl-dG and $N(7)$ -Methyl-G Adducts Following Low Dose $[D(3)]$ -Methylnitrosourea Exposures in Cultured Human Cells. *Chem. Res. Toxicol.* 27 (4), 480–482.
- (61) Kang, H., Konishi, C., Kuroki, T., and Huh, N. (1995) Detection of O^6 -methylguanine, O^4 -methylthymine and O^4 -ethylthymine in human liver and peripheral blood leukocyte DNA. *Carcinogenesis* 16 (6), 1277–1280.
- (62) De Bont, R., and van Larebeke, N. (2004) Endogenous DNA damage in humans: a review of quantitative data. *Mutagenesis* 19 (3), 169–185.
- (63) Tricker, A. R. (1997) N-nitroso compounds and man: sources of exposure, endogenous formation and occurrence in body fluids. *Eur. J. Cancer Prev.* 6 (3), 226–268.